ROM2F-88-022
September 1988

The deconfining phase transition in lattice gauge SU(3).

P. BACILIERI, E. REMIDDI, G. M. TODESCO

Infn - Cnaf and Dip. Fisica, Università di Bologna, 40126 Bologna, Italy

M. BERNASCHI, S. CABASINO, N. CABIBBO, L. A. FERNÁNDEZ*, E. MARINARI, P. PAOLUCCI, G. PARISI, G. SALINA, A. TARANCÓN†

Infn - Sezione di Roma, Gruppo Collegato di Roma II and Dip. Fisica, II Università di Roma, 00173 Roma, Italy

F. COPPOLA, M. P. LOMBARDO, E. SIMEONE, R. TRIPICCIONE

Infn - Sezione di Pisa, 56100 Pisa, Italy

G. FIORENTINI, A. LAI‡

Infn - Sezione di Cagliari and Dip. Fisica, Università di Cagliari, 91000 Cagliari, Italy

P. A. MARCHESINI

Cern, 1211 Geneve 23, Switzerland

F. MARZANO, F. RAPUANO, W. TROSS

Infn - Sezione di Roma and Dip. Fisica, Università di Roma La Sapienza, 00185 Roma, Italy

R. RUSACK

The Rockefeller University, New York, USA

ABSTRACT

By using a source method and improved measuring techniques, we study the decay of the Polyakov loop in $SU(3)$ lattice gauge theory at finite temperature. Our aim is to measure the correlation length of the system in the neighbourhood of the critical point. We work with lattices of size up to $16^2 \times 64 \times 4$. We found that the maximum correlation length is only bounded by the spatial dimension of the lattice. This result is the one expected in a second order phase transition and appears to be incompatible with the presence of the strong first order transition claimed in the literature.

Submitted to *Nucl. Phys.* B[FS]

* On leave from Universidad Complutense de Madrid. Partially supported by CAICYT Spain (AE86-0029). MEC fellow.
† On leave from Universidad de Zaragoza. Partially supported by CAICYT Spain. MEC fellow.
‡ Ing. C. Olivetti e C. S.p.a. fellow.

1. Introduction

The study of matter at high temperatures is the object of great interest since the existence of a new phase where quarks and gluons are not confined was predicted[1]. With the use of a lattice[2], a non perturbative treatment of the problem has become possible. The lattice regularization has allowed[3,4] to use strong coupling arguments in order to make plausible that confinement is indeed a low temperature phenomenon.

A rigorous proof of the existence of such a phase transition has been given in Ref. 5, but Monte Carlo simulations are the only effective tool one can use in order to get quantitative predictions. We want to learn, for example, the critical temperature T_c in the continuum limit and the order of the phase transition.

When matter goes from a phase where the interquark potential is linear to another where the quarks are unconfined, a strong change in the dynamical properties of the system is expected, with very important consequences in fields like Cosmology or Heavy Ions Collisions.

A complete study of this phenomenon requires the use of a theory where the dynamical fermions are present. This inclusion implies serious problems: theoretical (fermions in the lattice, existence of an order parameter for the transition,...) and numerical (algorithms, CPU time,...). Because of these problems, and the hope that the presence of dynamical fermions should not modify very much the scenario of pure gauge theory, the investigation has been addressed as a first step to the quenched theory. We hope to be able to extend the present investigation by including fermions in the near future.

Let us make clear that we will just be discussing pure gauge Quantum Chromodynamics, and we will not be interested in the effect of fermions. This is another interesting question, that we do leave open for the next future.

In lattice pure gauge $SU(2)$ the critical temperature and also the order of this transition seem clearly established both from theoretical and numerical results[6].

In $SU(3)$ after a great amount of numerical and analytical efforts, the knowledge of the nature of its transition, and especially its order, is an open question. In the literature a strong first order transition is usually assumed. In the case of small time dimension ($N_t = 2$) this behaviour has been supported by the results obtained in the Ref. 7. Nevertheless, in Ref. 8 The Ape Collaboration suggests a second order behaviour, and excludes a strong first order transition. In this paper we present a more detailed exposition of these results. The Columbia group has confirmed this development[9], by claiming, with a different approach, that the transition is not strong first order.

We have been motivated to study this problem by the following considerations:

i) Previous studies have often indicated slight changes of the critical temperature when different criteria are used. This is an indication that the transition is not so sharp.

ii) The Z_3 spin model in 3 dimensions, in the same universality class that $SU(3)$ gauge in 4 dimensions, was assumed to be of first order. However, universality arguments do not readily apply to the order of the phase transition: there are many cases in which a tricritical point separates a line of first order phase transitions from a line of second order phase transitions. It is also true that the order of the phase transition in Z_3 model is not definitively clear.

Up to now the study of the order of the deconfinement phase transition with Monte Carlo simulations was based on the quest for discontinuities of thermodynamical functions and metastabilities at the critical point. This approach has many problems as we will discuss below.

In this paper we present a very different approach. It principally consists in the measure of the correlation length ξ (or equivalently, the string tension, σ) close to the critical point, comparing the results from several lattice sizes. In a first order transition the correlation length remains finite in the neighbourhood

of the critical point, and we expect the correlation length to be a discontinuous function of the coupling when we go across the transition point. On the other hand, in a second order phase transition, the correlation length goes to infinity.

A computation of ξ in the neighbourhood of the transition has been followed in Ref. 10, but the improved techniques (smearing, source,...) we use, and the high statistics we can get, are crucial in allowing us to get good quantitative results.

Obviously, in a finite lattice the correlation length cannot exceed very much the lattice size, and also, discontinuities cannot be found. The point is that now it is possible to relate in a direct way the finite value of ξ with finite lattice effects. Indeed it is well known that at the critical point in a second order phase transition ξ is equal for large lattices to CL, where C is a constant (in the two dimensional models $C = \frac{1}{\pi\eta}$, η being equal to $\frac{1}{4}$ in the Ising model)[11] (See appendix B).

We try to avoid basing our conclusions in the observation of discontinuities since with a finite statistics in the neighbourhood of the critical point one might easily mistake an infinite derivative in the measured quantity for a discontinuity.

In section 2 we consider the generalities of the lattice approach to the study of $SU(3)$ gauge field theory at finite temperature, and we fix the notation. In §3 we define the measured observables and describe the techniques we used in order to obtain an improvement in the numerical results. In §4 we describe the Monte Carlo simulation. The methods for the analysis of data are considered in sections 5 and 6. The results are presented in §7. A discussion about the obtained results appears in §8.

2. Finite Temperature Lattice $SU(3)$

We define the $SU(N)$ gauge fields on a cubic four dimensional lattice with periodic boundary conditions. The partition function is

$$Z = \int dU \exp\left(-\beta \frac{1}{N} \sum_{n,\mu,\nu} \{1 - \Re \operatorname{Tr} U_{\mu\nu}(n)\}\right). \tag{2.1}$$

where $U_{\mu\nu}(n)$ is the ordered product of the four links of the plaquette in the μ-ν plane at the site $n = (x, y, z, t)$, and dU stands for the Haar measure over the SU(N) group extended over all links.

In order to formulate a field theory at finite temperature we consider an asymmetric box of size

$$L_x \times L_y \times L_z \times L_t, \tag{2.2}$$

where $L_t \ll L_x = L_y \ll L_z$. The system defined on such a lattice will be at a physical temperature $T = 1/L_t a$, with a the lattice spacing.

In this system an isolated static quark is represented as a current in the t direction which is closed by the boundary conditions. Then this static quark at the site n is described by the Polyakov Loop[3]

$$P(\vec{n}) \equiv \prod_{t=1}^{L_t} U_\tau(\vec{n}, t), \tag{2.3}$$

where U_τ is the link variable in the t direction, and $\vec{n} = (x, y, z)$. The free energy F_q of that state with respect to the vacuum, can be expressed in terms of the expectation value of P:

$$P = \frac{1}{NV_s} \Re \operatorname{Tr} \sum_{\vec{n}} \langle P(\vec{n}) \rangle = e^{-F_q/T}. \tag{2.4}$$

where V_s stands for the spatial volume. A situation where $P = 0$ corresponds to an infinite energy of an isolated static quark, and then, a confining phase. If an isolated quark has finite energy, we are in the deconfining phase, and $P \neq 0$.

This situation reflects the global Z_N symmetry of the model. The partition function is invariant under the global transformation

$$U_\tau(\vec{n},t) \to zU_\tau(\vec{n},t) \quad \forall\vec{n}, \tag{2.5}$$

where z is an element of Z_N, the center group of $SU(N)$, while P is not invariant under this transformation since

$$P(\vec{n}) \to zP(\vec{n}). \tag{2.6}$$

Therefore P is a true order parameter for this model.

When we consider this model near the critical point ($\beta \sim \beta_c$), the dynamics of the transition is dominated by an effective interaction between the Polyakov loop variables $P(\vec{n})$, which are close to a Z_N element. In this way the system is related with the Z_N spin model in 3 dimensions: they should be in the same universality class[12].

Universality arguments have been first advocated by Svetitsky and Yaffe[13] in order to support a first order phase transition in pure gauge $SU(3)$. This claim has received further support in Ref. 14, where the argument has been extended to the fermionic theory.

The problem is very specific to $N = 3$. In this case, in the Landau Ginsburg approach, if the field φ is proportional to the order parameter P, it is possible to write a non symmetry breaking φ^3 term in the Hamiltonian, and according to the Landau criterion this would produce a first order transition. The Landau criterion has also been applied to the three state three dimensional Potts model which should be in the same universality class. The order of the phase transition in this model has been (and is) very controversial (see for example Ref. 15 for detailed informations about different claims); ϵ expansion, mean field, Renormalization Group, cluster and $1/N$ techniques and Monte Carlo simulations do not lead to a clear cut conclusion about the order of the transition.

For example the Monte Carlo results of Ref. 16 conclude that a weak antiferromagnetic second nearest neighbour interaction, added to a first neighbour ferromagnetic term, leads to a second order phase transition, while the addition of a ferromagnetic second neighbour interaction leads to a first order one. Clearly if that would be the case all universality arguments would somehow not be of serious help. Indeed it is well known that there are transitions which change from first to second order when apparently irrelevant terms are added to the action. For example the finite range Z_3 model in $d = 2$ has a second or a first order transition as a function of the range of the interaction: if the interaction is short range (*i.e.* nearest neighbour), the transition is second order (as it can be verified by solving analytically the model); on the contrary, if the interaction has a very long (but finite) range the mean field approximation should be very accurate and the order of the transition should be the same of mean field, *i.e.* first order transition[15,16].

Other arguments used in order to claim that we are dealing with a first order phase transition are obtained with Monte Carlo simulations of lattice QCD. The first generation results that have been assumed to be relevant to the order of the phase transition are the ones of Refs.17 and 18. The most recent (and computationally intensive) work done about the pure gauge deconfinement transition[19–22] has assumed a first order transition.

The distinction between a first order and a second order phase transition is a delicate matter in general, particularly when the transition is of first order but there is a nearby second order transition, a case where the coherence length at the critical point (ξ_c) is rather large.

In most of the numerical simulations done for pure gauge QCD two different criteria were used to identify a first order transition: the presence of metastabilities near the critical point and the existence of discontinuities in the thermodynamical quantities.

The observation of metastabilities may hardly distinguish between a first

order transition and a second order one, especially if the quantity we consider has a behaviour like $|T - T_c|^{\widehat{\beta}}$, with a small exponent $\widehat{\beta}$. Indeed also near a second order phase transition the equilibration time is divergent and very long relaxation times are present. For example, simulations in the two dimensional Ising model, where the critical exponent for the magnetization, $\widehat{\beta}$, is equal to $\frac{1}{8}$ show *clear* signatures of metastability in numerical simulations (see appendix B). Moreover in a first order phase transition the correlation time τ increases (in three dimensions) as $\exp\left(A(L/\xi)^2\right)$, so that an observation of tunneling is itself an indication of large ξ ($\xi \sim L$), and is not connected with the order of the transition.

In principle the observation of discontinuities would be a very clear cut evidence for a first order phase transition. Unfortunately discontinuities can never be observed in finite volume simulations since the transition is rounded. Only a careful (not yet done for QCD) study of the dependence of the rounding with the volume can tell us if the rounding is going to disappear when the volume is going to infinite. We are working now in this direction[23].

As we have seen the different criteria used are intrinsically ambiguous: we firmly believe that the order of a phase transition can be determined numerically only by using finite size scaling analysis and by comparing the behaviour of the system at different L values. Most of the data published up to now can hardly be used to get firm conclusions about the nature of the transition because of the absence of any detailed comparison of results obtained on different finite volumes.

It should be stressed however that if the ξ_c is large it is impossible to distinguish a weak first order phase transition from a true second order unless we work on lattices of size L much greater that ξ_c. It is however remarkable that practically in all the cases known of weak first order transition associated to spontaneous symmetry breaking the transition may become second order by a small change in the Hamiltonian. In other words a large value of ξ_c is a very strong hint for the existence of a nearby tricritical point: beyond it the second

order transition should be present.

3. Source Method and Observables

3.1. Source Method

The *source* method we have used consists on the following: for $z = 0$ we fix all links in the x, y, t directions to the identity (*cold wall*). This can be thought as a perturbation of the system at $z = 0$, which propagates in the z direction.

This is one of the procedures that are normally used in Statistical Mechanics; in this way we choose, in the phase in which the symmetry is spontaneously broken, a preferred vacuum: between the three possible vacuum states, with

$$\arg(P) = \frac{2\pi}{3}n, \quad n = 0, 1, 2 \tag{3.1}$$

we select in this way the $n = 0$ state. Therefore the source method avoids the tunnelling problems (for external *magnetic* field equal to zero), and also generates a very strong signal that will enable us to measure the string tension at large distances from the wall. This method has been quite useful for measuring the string tension in the zero temperature limit.

We can think of this system as a tridimensional one where in each site we have defined the $P(\vec{n})$ variable; then on the wall P is the identity matrix. In a x-y plane, we define

$$C(z) = \frac{1}{L_x L_y} \Re \operatorname{Tr} \sum_{x,y} \langle P(x, y, z) \rangle. \tag{3.2}$$

With $C(z)$ we can extract the energy cost to have a quark at distance z from the wall. We can write

$$C(z) = e^{-V(z)/T}, \tag{3.3}$$

where $V(z)$ is the interquark potential summed over a plane.

In the unbroken phase $V(z)$ grows linearly at large distances, and we define σ as the corresponding coefficient

$$V(z)a = \sigma L_t z, \tag{3.4}$$

therefore the correlation length in lattice units is defined as

$$\xi = \frac{1}{\sigma L_t}. \tag{3.5}$$

In the unbroken phase

$$C(z) \underset{z\to\infty}{\sim} Ae^{-z/\xi}, \tag{3.6}$$

and the influence from the source disappears for large z.

In the broken phase $C(z)$ is non zero at infinite z, and the argument of P is zero. Now $V(z)$ is constant for large z, and this means that it is possible to have a isolated external quark with a finite energy cost. In this case

$$C(z) = Ae^{-z/\xi} + B, \tag{3.7}$$

where B, which we call *background* (or equivalently the order parameter), is the value of P in absence of wall (when the system is spontaneously broken to the $n = 0$ state).

We can characterize $1/\xi$ as the energy of the lowest state which transforms under a non trivial representation of the gauge group. The cold wall gives a stronger signal than what can be measured by studying loop-loop correlation functions, but also introduces a strong distortion at short distance from the source. This problem can be avoided just going to large distances from the wall. We remark that the problem of the high energy fluctuations at small distances is also present when measuring loop-loop correlation functions. Although the contribution of excited states is smaller for the latter, the weakness of the signal

makes it very difficult to find an asymptotic behaviour, especially if the correlation length is large. Another fundamental advantage of the source method is that, by avoiding the tunnelling, (in the phase where $B \neq 0$) it improves the thermalization speed.

3.2. Smearing

Even if the source method allows us to measure at large distances from the wall, it is very important to reduce as much as possible the effect of the short distance fluctuations in the measures: these fluctuations correspond to states of high energy in the transfer matrix approach. The general goal of the smearing procedure is to reduce the projection of the measured operators over the high energy states and to enhance the projection over the low energy states we want to measure.

Let us describe the smearing procedure[24] we use. We generate a sequence of links, $U_\mu^{(s)}$, in the hyperplane $z = constant$ such that $U_\mu^{(1)}$ is the standard link variable, and

$$U_\mu^{(s+1)} = \Pi\big(U_\mu^{(s)} + \epsilon \sum_{\eta=1,-1} \sum_{\nu\neq\mu} S_{\mu\nu}^{\eta}\big), \tag{3.8}$$

where $S_{\mu\nu}$ is the staple (incomplete plaquette) for the link μ in the ν direction (along x, y or t), with orientation η, and $\Pi(A)$ stands for a projection of A over a $SU(3)$ element. We use the projector ($\vec{b}' \equiv \vec{b} - (\vec{a}^* \cdot \vec{b})\vec{a}/|\vec{a}|^2$)

$$\Pi\begin{pmatrix} \vec{a} \\ \vec{b} \\ \vec{c} \end{pmatrix} = \begin{pmatrix} \vec{a}/|\vec{a}| \\ \vec{b}'/|\vec{b}'| \\ \vec{a}^* \times \vec{b}'^*/(|\vec{a}||\vec{b}'|) \end{pmatrix} \tag{3.9}$$

This is not the only procedure to define $\Pi(A)$ but the actual selection is not very important in a Monte Carlo simulation. It is also is clear that $\Pi(A)$ is well defined only if $\vec{a}$, $\vec{b}$ and $\vec{a} \times \vec{b}$ are not zero. This is guaranteed if ϵ is small enough because in this case the argument of Π in (3.8) is close to one $SU(3)$ element.

If the global Z_3 transformation (2.5) is made it is easy to check from (3.8) that

$$U_\tau^{(s)}(\vec{n},t) \to z U_\tau^{(s)}(\vec{n},t) \quad \forall s,\vec{n}. \tag{3.10}$$

Therefore the smearing procedure preserves the Z_3 symmetry, that is to say, the symmetry properties under Z_3 are the same for all the smearing numbers.

With smeared links we construct the smeared operators, for instance

$$p^{(s)}(\vec{n}) \equiv \prod_{t=1}^{L_t} U_\tau^{(s)}(\vec{n},t), \tag{3.11}$$

verifying

$$p^{(s)}(\vec{n}) \to z p^{(s)}(\vec{n}) \tag{3.12}$$

therefore the corresponding $P^{(s)}$ from (2.4), is a good order parameter for all s.

The smearing procedure averages the gauge fields with the neighbouring fields. After s steps the $U^{(s)}$ variables contain information up to $\sim 2^s$ distances. In this way the short wavelength fluctuations in the gauge fields are suppressed.

The smearing is very useful, but is also very time consuming. The computer time for each smearing step is of the same order as the time needed to perform a Monte Carlo iteration. This situation worsens when the correlation length is large, because in this case in order to obtain a *smoothing* of the irregularities at small scale we must go to very large distances in the lattice, and then a large number of smearing steps is needed (notice that even if some information is propagated at a distance which is exponentially large in the smearing number, the effective propagation distance behaves as $\sqrt{s}^{[24]}$).

3.3. BLOCKING

We have found that the overhead due to the computation of the smeared variables can be alleviated very easily with a *blocking* procedure.

In the course of the measurement, after s_0 smearing steps, at a fixed z, we can transform the tridimensional lattice into a smaller one:

$$L_x \times L_y \times L_t \to \frac{L_x}{2} \times \frac{L_y}{2} \times \frac{L_t}{2}. \tag{3.13}$$

We can define the link variables, $W_\mu(\vec{n};t)$, in this coarse grained lattice, in terms of the variables on the original lattice, $U_\mu^{(s_0)}(\vec{n};t)$, by

$$W_\mu(\vec{n};t) = U_\mu^{(s_0)}(2\vec{n};t)\; U_\mu^{(s_0)}(2\vec{n}+\vec{\mu};t). \tag{3.14}$$

$\vec{n}$ runs on the coarse grained lattice, and μ runs in the x, y, or z direction. After this step we continue with the usual smearing procedure but on the smaller lattice fields. In order to make the notation simple we just add 1 to the smearing index when the blocking is made ($U_\mu^{(s_0+1)}(\vec{n},t) \equiv W_\mu(\vec{n},t)$). We remark that the transformation (3.14) preserves the Z_3 structure.

Notice that when the blocking procedure is performed, we disregard $\frac{3}{4}$ of the total number of variables in the $z = constant$ plane. We found that, after few smearing steps we can reduce the lattice size in this way with a negligible loss of information, since now every link contains information about its neighborhood. The computer time required to perform a smearing step in the blocked lattice is 8 times smaller.

4. Monte Carlo Simulation

For this simulation 4,500 hours of a 256 Mflops Ape computer[25] have been used. We have updated our gauge field configurations by using an overrelaxed updating method[26,27]. With the code used the updating time is of 30 μs per link. We have chosen this method because of its great speed and efficiency in the updating process[28,29]. In order to control that the results we have obtained are *method* independent we have done some test runs using the Metropolis and the Quasi Heat Bath methods[30]. The results are fully compatible.

We have used three different lattice sizes:

$$\begin{aligned} &8^2 \times 32 \times 4, \\ &12^2 \times 48 \times 4, \\ &16^2 \times 64 \times 4, \end{aligned} \tag{4.1}$$

in order to control the evolution of the relevant quantities when the lattice size is increased. Notice that we limit ourselves to study $L_t = 4$ systems, therefore our conclusions about the order of the deconfining transition strictly applies only for this case.

In the smaller lattice we studied 16 different β values, from 5.620 to 5.730, with a more dense distribution close to β_c. On the $12^2 \times 48 \times 4$ lattice we have considered 5 different values between 5.675 and 5.695, and on the $16^2 \times 64 \times 4$ lattice we have worked at $\beta = 5.690$. We have performed a larger number of MC iterations close to β_c, measuring in all cases every 10 sweeps. In the smaller lattice we have carried out up to 170,000 iterations for some values of β, discarding 7,000 sweeps for thermalization. In the $12^2 \times 48 \times 4$ we have performed 10,000 Monte Carlo steps for thermalization and then up to 240,000 for each β. On the $16^2 \times 64 \times 4$ we have thermalized with 20,000 iterations, with a total of 150,000 Monte Carlo iterations. Let us describe the protocol of our measures. Every 10 whole sweeps, for every value of z, first we measure the Polyakov Loop with the *true* link variables ($s = 1$). Then one smearing step is performed, measuring the

observables with $s = 2$; we block the lattice and we measure in these *blocked* variables, calling $s = 3$ the corresponding observables. Thereafter, we repeat 8 smearing steps in the coarse grained lattice. The total computer time taken by the whole procedure is equivalent to that of 2 smearing steps done on the original lattice. We take $\epsilon = 0.2$ in (3.8).

5. Effective mass analysis

The first analysis we have done in order to extract the correlation length, is based on the effective mass estimator at a given smearing number s for every time. It is defined by looking at the variation of the signal from the wall between two successive z slices. We call *effective mass*, $m^{(s)}(z)$, the solution of the equation

$$\frac{\cosh\Big((L_z/2 - z)m^{(s)}(z)\Big)}{\cosh\Big((L_z/2 - (z+1))m^{(s)}(z)\Big)} = \frac{C^{(s)}(z)}{C^{(s)}(z+1)}, \tag{5.1}$$

which we solve numerically.

In the region where $B = 0$ this gives a precise determination of the string tension, by means of the asymptotic behaviour of $m^{(s)}(z)$ for large z. Close to the critical point (small σ) the excited states give an important contribution to $C^{(s)}(z)$ and we need to go to very large z and s in order to obtain an asymptotic behaviour for σ. A independence of $m^{(s)}(z)$ with respect to s and z is a clear signal that this asymptotic behaviour is reached. We call m to this asymptotic value, so $\xi = 1/m$ or $m = \sigma L_t$ in lattice units.

The fluctuations of $C^{(s)}(z)$ close to the walls are very small and they have a very high frequency. For very large z these fluctuations are bigger with lower frequency. The fluctuations of $C^{(s)}(z)$ and $C^{(s)}(z+1)$ are in any case highly correlated, yielding smaller fluctuations in the ratio (5.1). As a consequence, the errors on $m^{(s)}(z)$ are relatively small.

In the region where $B \neq 0$, $m^{(s)}(z)$ from (5.1) is no longer a good estimator for σ. In fact, in this region we find a decreasing $m^{(s)}(z)$ when z is increased, as a signal of a background. In this way we have a precise determination of σ in the unbroken phase and also a method to find the value of β where the background begins to be non zero (critical point). We stress that the use of $C^{(s)}(z)$ allows us to work with a very large set of operators (s different operators) in the σ channel, which allows us to check if the results we obtain do not depend on the operator we consider.

In fig. 1 we give a typical example of what we mean by an asymptotic behaviour of the result. For $\beta < \beta_c$ in the $8^2 \times 32 \times 4$ lattice we plot the effective string tension at different z versus the operator considered. The operator is plotted as a function of the inverse of the smearing number. The points at $s = 1$ are the ones we would get by considering the usual Polyakov loops. The results from (5.1) for $m^{(s)}(z = 0)$ are strongly dependent of the choice of operator (smearing number). For increasing z the result is less dependent on s. Because of the smallness of the *mass* of the excitations we are considering, in order to obtain an asymptotic behaviour we need to go to distances bigger than 5 to obtain an approximate constant value of $m^{(s)}(z)$ and for this z the effective mass is s independent. The crossing of two different curves for operators with $s \sim 8$ can be interpreted as a change of sign of the coefficient of the first excited state.

Another way to measure the mass looking at the mass estimators $m^{(s)}(z)$ is summarized in fig. 2. Every line joins the effective masses with the same smearing s for different distances. The large fluctuations for small s and z disappear when these are increased, and we obtain a plateau (s and z independence) as a clear sign for the asymptotic behaviour and also of the absence of background.

6. Global fit analysis

The main lack of an effective mass analysis is that it considers just two z values to construct the estimator. So it does not use *at once* all the information we have.

To take simultaneously into account the information of all distances, we perform also global fits to the function:

$$C^{(s)}(z) = A^{(s)} \cosh\Big(m^{(s)}(\frac{L_z}{2} - z)\Big) + B^{(s)} \tag{6.1}$$

for a given s. Notice that A and B are smearing dependent, but $m^{(s)}$ should not be. The high statistics used makes all the distances (up to 48 different points) significative, because of the small decay of the signal (small m) in the β region we are studying.

We realize that the results from the global fit analysis are less accurate than those obtained from an effective mass estimation. Nevertheless, a global fit has some interesting features. The fact that a global fit takes into account all the useful points allows us to make a test of consistency with the behaviour reported in (6.1). In fig. 3 we show an example of a very good agreement with a hyperbolic cosinus behaviour.

But the most interesting point is that this method allows us to compute the mass even when $B^{(s)} \neq 0$, as well as the numerical value of $B(s)$, which we cannot calculate with a standard effective mass analysis. This offers a somewhat independent method to calculate β_c.

The main problem with global fitting is that the functional behaviour is given *a priori*. When a mass estimator is constructed by using just two successive z values, it is very easy to control when the excited states do not contribute to the decay of $C^{(s)}(z)$, just by comparing $m^{(s)}(z)$ at different distances and smearing numbers. Now the situation is more involved because we have only one mass parameter to fit for all values of z.

Let us call $d_{\min}$ the first distance we include in the fit, that is to say, we consider in the fit all z slices with $d_{\min} \leq z \leq L_z - d_{\min}$. If the fit is made with all distances ($d_{\min} = 0$), it is clear that the small distances, with much smaller error, have an important weight in χ^2 (see appendix A), and since the decay at these small distances is governed by the excited states, the obtained mass will be overestimated. When $d_{\min}$ is increased, the obtained mass will be smaller. On the other hand, for large $d_{\min}$, the error in $m^{(s)}$ becomes very large.

Fortunately, the smearing procedure helps us to find an asymptotic behaviour. When we do not discard a number of z slices large enough, we find a smearing dependence of the fitted parameters. On the other hand, a smearing independence of the results would mean that the obtained data are asymptotic. We have checked that this property holds in all cases. In fig. 4 we show an example of both situations. The number of points we have discarded is typically 6 (after summing the measures from both sides of the wall), for instance we use the measurements from distance 7 to distance 24 from the wall. As will be show below, an estimation obtained with the data at small distances suffers from the contribution of higher excited states and the obtained results would be very different.

The strategy we have followed is to carry out first a 3 parameter fit, and in the cases where the background was found compatible with zero, we have repeated the fit with just two parameters. In this way we can obtain a more precise result for m in the region where $B^{(s)} = 0$.

Regarding to the results for the masses we obtain compatible results in all cases where the effective mass calculation is possible ($\beta < \beta_c$). In the next chapter we will comment the results in more detail.

Let us focus our attention on the estimation of the background $B^{(s)}$. First of all we note that the background is a smearing dependent quantity, so, we do not expect a similar behaviour to that of the correlation length. We find than the background grows up very fast with the smearing number. However, the *smeared*

Polyakov Loop $P^{(s)}$ is an order parameter as good as the usual Polyakov Loop. We recall that the background at a given smearing number $B^{(s)}$ is just the value of $P^{(s)}$ at infinite distance from the wall, *i.e.* the *spontaneous magnetization* or mean value of the Polyakov Loop. As the symmetry properties of $P^{(s)}$ are smearing independent we expect that the critical behaviour for all s will be similar.

In fig. 5 we show how the presence of a background is easily recognizable with a global fit.

Unfortunately, in the broken phase, and for β close to β_c, a precise estimation of the correlation length is extremely difficult, because it is not easy to determine which amount of signal comes from the wall and what is true background. A bit far from the critical point (at $\beta/\beta_c \sim 1.005$, for example) the determination of the background is very good, but its value is large, so the signal from the wall is lost in the background at relative small distance and it is necessary to compute the correlation length without discarding many distances. Fortunately, the asymptotic behaviour in this case is found at a not very large distance.

7. Results

In this section we present a more detailed discussion of the results obtained in this paper, see table 1 and figs. 6 and 7.

First let us comment on the precise determination of the critical point. Since all $B^{(s)}$ have the same symmetry properties under the center group, this β value is s independent. The important point is that with the source method $B^{(s)}$ is not necessarily zero in a finite lattice, and it is not necessary to impose unphysical prescriptions in order to extract the critical point. Also, at the critical point the correlation length is expected to be maximum, and this fact offers another independent criterion to find β_c.

It is very important to have *physical criteria* in order to determine β_c, because unphysical ones can introduce uncontrollable ambiguities. The determination of

the transition point with a criterion as the number of elements which are *close* to a center element is somewhat arbitrary, and by modifying this number of elements we obtain different values of β_c. The value we have found for β_c is compatible with those obtained by using more standard methods, however our results are very precise and they do not suffer from these ambiguities.

In the $8^2 \times 32 \times 4$ lattice the first apparition of background is not clear since even if the wall is present, the tunnelling effects are not absolutely excluded in such small lattice: even a bit over the critical point a global fit with large $d_{\min}$ is possible with $B = 0$. In fact for $\beta = 5.695$ the effective mass has the $B = 0$ behaviour but with a large error. A global fit with not very large $d_{\min}$ shows that a small background is necessary to obtain an acceptable fit.

When the $12^2 \times 48 \times 4$ lattice is used the situation is very much clearer. The effective mass is not asymptotic, and also a global fit shows a clear background. This is a clear evidence that the tunnelling effects are negligible in this lattice.

In the $16^2 \times 64 \times 4$ lattice at $\beta = 5.690$ we find with the effective mass analysis a clear asymptotic mass, and a global fit also shows that the background is zero (see fig. 8).

For β values larger than 5.695 we found, both from global fits or effective mass analysis, a very clear presence of a background (see fig. 5). We remark that the nonzero value of $B^{(s)}$ for β close to β_c followed by a slow increase as a function of β (see fig. 7) far from being a *proof* of a discontinuity, it is the predicted value for a behaviour of type

$$B^{(s)} = B_0^{(s)}(\beta - \beta_c)^{\widehat{\beta}}, \tag{7.1}$$

with the critical exponent $\widehat{\beta}$ s-independent, since the smearing process preserves the global Z_3 symmetry. Unfortunately a determination of the numerical value of $\widehat{\beta}$ has been impossible. We only can say that its value lies in the interval $[\frac{1}{6}, \frac{1}{3}]$, and the value of $B_0^{(s)}$ is of the order of 1. We remark that a direct determination

of this exponent is extremely difficult because of the infinite derivative of $B(\beta)$ at the critical point, and the fact that $B^{(s)}$ becomes large very fast; so, nonlinear effects that deviate from (7.1) are expected also for β near β_c.

Let us now comment on the variation of the *mass*, m with β. We observe several facts:

i) m, decreases as β goes from 5.620 to 5.690. However, for $\beta > 5.690$ the *mass* grows with β, but without any evidence of discontinuous behaviour.

ii) As β goes to 5.690 m decreases with an increasing rate (derivative more negative). There is an approximate inflexion point at $\beta = 5.675$ for the $8^2 \times 32 \times 4$ lattice, for which the correlation length ξ becomes ~ 6 in lattice units.

iii) The deviation of the results for the two smaller lattices increases with β in the interval $[5.675, 5.690]$.

iv) The main point is that for all lattices the value of the correlation length at $\beta = 5.690$ is of the order of the spatial size.

All these results support the conclusion that all the contribution to m in the neighbourhood of $\beta = 5.690$ comes only from the finite size effects present in a second order transition. In this case there is a region in the neighbourhood of the critical point where ξ is arbitrarily large. In a finite lattice (of size L_x in the transversal spatial direction), in the β region where $\xi > L$ in the infinite lattice, the inverse of the correlation length cannot decrease, so a *plateau* in this region is expected.

Thus the true correlation length at β_c, that is, the correlation length for an infinite lattice must be much greater than the values we found. It is difficult to accept that such a large value for ξ has a physical meaning, even more if we take into account that a value for ξ greater than 16 corresponds to an energy less than 100 MeV. The existence of this small mass scale would be very surprising. It is a much more natural interpretation to suppose that the large value obtained for ξ

is a manifestation of a divergent value in the $L_z \to \infty$ limit. This suggest that the deconfinement phase transition in pure lattice QCD is second order. In addition we note that the ratio between the maximum correlation length measured on the $L_z = 12$ and the $L_z = 8$ lattice is

$$\frac{\xi_{L_z=12}}{\xi_{L_z=8}} = 1.42(18), \tag{7.2}$$

in agreement with the finite size scaling prediction (12/8) for a second order phase transition. For $L_z = 16$ we obtain a greater value of ξ but surely not the greatest for this lattice. This is a normal fact because an infinite derivate for m in β_c in the thermodynamical limit, would produce in such a big lattice very strong changes in m for very small changes in β. Then (remember that we have run just at $\beta = 5.690$) a bit above 5.690, ξ should be increased (see fig. 6). At this point we can affirm that β_c is between 5.690 and 5.694.

Finally let us note that in a first order phase transition, a discontinuity in the quantities corresponding to excited states is also expected. In fig. 9 we show the effective mass for $s = 1$ at distance 1 and 2, whose behaviour is strongly dependent on excited states. We do not see any discontinuity when crossing the critical point. Another possible interpretation of this figure (if we consider only $\beta \leq \beta_c$) is that if we compute m without smearing, and using only small distances, the transition behaves as a first order one. See also in fig. 10 how the use of points at small distance from the wall for the non smeared operators ($s = 1$), modify very much the results for m specially for β very close to β_c. For these β values if a smaller number of points in the z direction is significative, and we assume that $B = 0$, then m is large, with a large χ^2. On the contrary, if we assume $B \neq 0$, then a fit with a large m and B is possible with a relatively acceptable χ^2. Nevertheless, our statistical errors allow us to know that such fits are wrong, but with larger errors it would be impossible to see that the measured ξ is not correct.

Summarizing, we conclude that we have not found any evident sign of discontinuities to indicate that the deconfining phase transition in pure QCD is a

first order one. All the "sharpness" we found can be interpreted as the effect of the discontinuity in the derivative, or of a divergence in the correlation length, properties expected in a second order phase transition. Our main result is the precise measure of the correlation length in the neighbourhood of the transition. We have measured values of this quantity very much greater than all the ones measured until now. The behaviour of ξ_c, with the finite size scaling analysis we made, fully corresponds to that expected in a second order phase transition. We cannot affirm categorically that the transition is second order, since it is always possible to have a first order transition with a very large correlation length at the critical point, although the properties of such a "weak first order transition" would be very similar to those of a second order one, both from theoretical and experimental points of view. Also, its small discontinuity would surely disappear by the effect of dynamical fermions that seems to smooth the phase transition. We believe that the deconfinement phase transition in full QCD is not first order.

Acknowledgements:

We would like to thank T. Banks, U. Marini Bettolo, R. Medina, S. Shenker and A. Ukawa for useful discussions.

APPENDIX A

We discuss in this appendix the error analysis we have done. The first problem we have to face for a reliable error analysis is related with the correlations between successive Monte Carlo configurations. This correlations remain after a very large number of sweeps in the neighbourhood of the critical point. To control this problem, the error analysis has been carried out by using large bins of data of about 10,000 Monte Carlo sweeps. We have confidence that this bin length is large enough to get a good estimation of the errors. We have performed some test to confirm this assumption.

As an example, in fig. 11 we show a typical example of a Monte Carlo evolution near the critical point. Because of the presence of the wall, where $P(\phi)$ is the

identity matrix, the phase of the Polyakov loop is zero at small distance d, that is to say, is very close at the unity of the center of $SU(3)$. For increasing d, the system can fluctuate, and close to the critical point, these fluctuations are very strong, because the system jumps suddenly between the 3 elements of Z_3. This fact occurs when we move in the Monte Carlo *time*. If β is very close to β_c these fluctuations have a very large mean life, which is, a metastable-like behaviour, similar to that found in the Ising Model (see Appendix B), and then properly we can properly call it "critical slowing down". We see fluctuations with mean life of some thousands of sweeps. Nevertheless the whole figure corresponds just to 30,000 from the 200,000 iterations used in the analysis.

The second problem is related with the correlations between measures corresponding to different physical distances. The different points are not independent, but strongly correlated. In the effective mass analysis we have considered this effect by directly computing the correlation between successive measures $\langle \varsigma_z \, \varsigma_{z+1} \rangle$, where $\{\varsigma_z\}$ are the data coming from the simulation.

To take into account this correlation in the global fits we have defined the χ^2 function in terms of the full covariance matrix,

$$\chi^2 \equiv \frac{1}{N_{\text{points}} - N_{\text{parameters}}} \sum_{z,z'} (C(z) - \varsigma_z)(C(z') - \varsigma_{z'}) V^{-1}_{zz'}, \qquad \text{(A.1)}$$

$$V_{zz'} \equiv \langle \varsigma_z \, \varsigma_{z'} \rangle - \langle \varsigma_z \rangle \langle \varsigma_{z'} \rangle. \qquad \text{(A.2)}$$

In practice, to be closer to a gaussian behaviour, we have summed the two measures corresponding to the same z distance from the wall (from both sides), however we show independently all of them in the figures.

Notice that the usual approximation $V_{zz'} \sim (\langle \varsigma_z^2 \rangle - \langle \varsigma_z \rangle^2)\delta_{zz'}$ neglects the correlation between measures at different z, and this means an underestimation in the value of χ^2. This would make impossible the computation of the error in the fitted parameters just by looking at the variation of χ^2. We remark again

that this problem is particularly important in the neighbourhood of the critical point, where there are long range correlations.

APPENDIX B

In this appendix we want to show how the source method we use works in a model where the exact solution is known, and also to discuss whether a very popular criterion, the existence of metastability, is relevant to distinguish a first order transition from a second order one. To do that we consider the two-dimensional Ising model, whose partition function is defined as

$$Z = \sum_{\{C\}} \exp\left(-\beta \sum_{i,j} \sigma_i \sigma_j\right), \qquad \text{(B.1)}$$

which has a second order transition at $\beta_c = \log\left(1 + \sqrt{2}\right) = 0.88137\ldots$.

The correlation length at β_c is infinite, since the correlation between spins has not an exponential decay. However, in a $L \times \infty$ lattice the decay has an exponential tail[3], with a mass $m(L) = \frac{\pi}{L}\eta$, where η is a critical exponent ($\eta = \frac{1}{4}$).

We carry out a Monte Carlo simulation to find this mass in a finite lattice. To do that we use a 40×120 lattice with periodic boundary conditions, and a cold wall ($\sigma_{z=0} = \sigma_{z=L_z} = 1$). The method used is a Heat Bath one. We have run 8×10^6 Monte Carlo iterations, and we have fitted the correlation from the wall as in the $SU(3)$ case. Very close to the critical point from below, $\beta = 0.8813$, we found that $B = 0$ and $m = 0.019(3)$ (see fig. 12), in very good agreement with the exact result $m_{\text{exact}} = 0.0196$. In the broken phase ($\beta = 0.89$) we find also the correct values for the mass and the background.

We conclude that the source method works very well to measure large correlation lengths in the two dimensional Ising Model. The discrete nature of spins in the Ising model imposes the use of a very large statistics. For example, for a good fit we have to discard all distances from the wall lower than 15.

Now we want to see what happens when a standard criterion like metastability is used in a similar lattice. We run 10^5 Monte Carlo iterations in a 40^2 lattice and measure the magnetization for every configuration. The result at $\beta = 0.8814$ can be seen in fig. 13. We repeat this calculation modifying β (always close to β_c), also using different random number generators, and with a different updating algorithm (Metropolis). The result is always the same. This *anomalous metastability* can be understood very easily by considering the behaviour of the magnetization close to the critical point. In the Ising model, for $\beta > \beta_c$

$$\langle\sigma\rangle = C(\beta - \beta_c)^{1/8} \qquad \text{(B.2)}$$

with $C = (4\sqrt{2})^{1/8} = 1.24185\ldots$ and then at a distance from β_c of 3×10^{-5}, $\langle\sigma\rangle = 0.3$. Therefore, as far as the numerical simulation is concerned, the system cannot distinguish this small interval, and fluctuates as if the transition were first order. In conclusion, in the neighbourhood of the critical point, when the critical exponent is very small, a *metastability* is possible, and then this criterion is not definitive for establishing the order of the transition.

REFERENCES

1. N. Cabibbo and G. Parisi, *Phys. Lett.* **59B**(1975), 67.
2. K. G. Wilson, *Phys. Rev.* **D10**(1974), 2445.
3. A. M. Polyakov, *Phys. Lett.* **72B**(1978), 477.
4. L. Susskind, *Phys. Rev.* **D20**(1979), 2610.
5. C. Borgs and E. Seiler, *Nucl. Phys.* **B215[FS7]**(1983), 125;
   C. Borgs and E. Seiler, *Commun. Math. Phys.* **91**(1983), 329.
6. J. Engels et al., *Nucl. Phys.* **B280[FS18]**(1987), 577.
7. M. Karliner,S. Sharpe and Y. F. Chang,, *Nucl. Phys.* **B302**(1988), 204.
8. The Ape Collaboration, P. Bacilieri et al.*preprint* ROM2F/88/020, June 1988. To appear in Phys. Rev. Lett.
9. F. R. Brown et al., *preprint* CU-TP-407, August 1988.
10. M. Fukugita, T.Kaneko and A. Ukawa, *Phys. Lett.* **154B**(1985), 185.
11. J.L. Cardy, *J. Phys.* **A17** (1984), L385
12. G. Parisi, *Statistical Field Theory*, (Addison Wesley, 1988)
13. L. G. Yaffe and B. Svetitsky, *Phys. Rev.* **D26**(1982), 963;
    B. Svetitsky and L. G. Yaffe, *Nucl. Phys.* **B210[FS6]**(1982), 423.
14. T. Banks and A. Ukawa, *Nucl. Phys.* **B225[FS9]**(1983), 145.
15. F. Y. Wu, *Rev. Mod. Phys.* **54**(1982), 235.
16. F. Fucito and A. Vulpiani, *Phys. Lett.* **89A**(1982), 33.
17. J. Kogut et al., *Phys. Rev. Lett.* **50**(1983), 393.
18. T. Çelik, J. Engels and H. Satz, *Phys. Lett.* **125B**(1983), 411.
19. A. D. Kennedy, J. Kuti, S. Meyer and B. J. Pendleton, *Phys. Rev. Lett.* **55** (1985), 1958.

20. S. A. Gottlieb, J. Kuti, D. Toussaint, A. D. Kennedy, S. Meyer, B. J. Pendleton and R. L. Sugar, *Phys. Rev. Lett.* **55** (1985), 1958.

21. N. H. Christ and A. E. Terrano, *Phys. Rev. Lett.* **56** (1986), 111.

22. N. H. Christ, *Nucl. Phys. (Proc. Supp.)* B4(1988), 241.

23. The Ape Collaboration, *work in progress*

24. The Ape Collaboration, M. Albanese et al., *Phys. Lett.* B192(1987), 163.

25. The Ape Collaboration, M. Albanese et al., *Comp. Phys. Comm.* 45(1987), 345.

26. M. Creutz,, *Phys. Rev.* D36(1987), 515.

27. F. R. Brown and T. J. Woch,, *Phys. Rev. Lett* 58(1987), 2394.

28. M. Bernaschi and L. A. Fernández, *preprint* ROM2F/88/002, January 1988. To appear in Phys. Lett. B

29. R. Gupta et al. *preprint* LA-UR-88-824, March 1988.

30. N. Cabibbo, E. Marinari, *Phys. Lett.* 119B(1982), 387.

TABLE CAPTIONS

1: Summary of the results obtained for the correlation length and spontaneous magnetization in all the considered lattices.

FIGURE CAPTIONS

1) A typical example of crossing ($8^2 \times 32 \times 4$ lattice at $\beta = 5.680$) The lines correspond to different distances. The gap between $s = 1$ and $s = 3$ is an effect of the *blocking* procedure described above. The crossing point at $s \sim 8$ is due to the change of the sign of the contribution of the first *excited state*.

2) Mass estimator as a function of the distance from the wall in a $8^2 \times 32 \times 4$ lattice at $\beta = 5.680$. The different lines correspond to different smearing numbers. We plot error bars for $s = 11$

3) Global fit in the $8^2 \times 32 \times 4$ lattice at $\beta = 5.680$ discarding the points nearer than 5 lattice units from the wall.

4) Fitted mass, $m^{(s)}$, as a function of the smearing. The solid (dashed) line has been obtained discarding the points at a distance $d < 5$ ($d < 3$).

5) $C^{(6)}(z)$ for a $12^2 \times 48 \times 4$ lattice at $\beta = 5.695$. The solid (dashed) line corresponds to a fit with free (fixed to zero) background. The presence of the background is unavoidable to make a good fit.

6) Results for the mass, or inverse correlation length, as a function of β. The squares correspond to the $8^2 \times 32 \times 4$ lattice, the circles to the $12^2 \times 48 \times 4$ one and the cross to the $16^2 \times 64 \times 4$ one. The dashed line represents a function of type $|\beta - \beta_c|^\nu$, with $\beta_c = 5.691$ and $\nu \sim 1/2$.

7) Background as a function of β, for the $8^2 \times 32 \times 4$ lattice (squares), and the $12^2 \times 48 \times 4$ one (circles). As a possible interpretation of the data, we plot a fit to $(\beta - \beta_c)^{\widehat{\beta}}$ obtained by fixing $\beta_c = 5.691$ and $\widehat{\beta} = 1/5$ (dashed line).

8) As in fig. 2 for $\beta = 5.690$ in the $16^2 \times 64 \times 4$ lattice.

9) Effective mass with $s = 1$ at $z = 1$ (squares for $8^2 \times 32 \times 4$ and circles for $12^2 \times 48 \times 4$) and $z = 2$ (crosses for $8^2 \times 32 \times 4$ and rhombs for $12^2 \times 48 \times 4$), as a function of β. For these z values the contribution of excited states are dominant.

10) Global fits for $C^{(1)}(z)$ in the $12^2 \times 48 \times 4$ at $\beta = 5.690$. The solid line stands for the best fit ($B = 0$, $d_{\min} = 6$), the dashed line for a fit with B fixed to 0 and $d_{\min} = 3$, and the dotted line also with $d_{\min} = 3$ but with B free in the fit.

11) Phase of the Polyakov Loop summed over the x-y plane, as a function of z and the Monte Carlo iteration in a $12^2 \times 48 \times 4$ lattice at $\beta = 5.690$. The lines for fixed z represent the average over 100 contiguous measures taken every 10 sweeps. The data shown corresponds to three bins of 10,000 iterations from the total of 20 used in the error analysis.

12) Fit for the magnetization of the line z in the two dimensional Ising model at $\beta = 0.8813$ in a 40×120 lattice with a cold wall (all spins fixed to 1) at $z = 0$, with periodic boundary conditions.

13) Magnetization versus the Monte Carlo iteration for the Ising Model in a 40×40 lattice at $\beta = 0.8814$. A single point is the mean magnetization over 5 succesives configurations.

L_z	β	$\xi^{(I)}$	$\xi^{(II)}$	B
$8^2 \times 32 \times 4$	5.620	2.4(2)	2.3(2)	—
"	5.630	2.6(3)	2.24(11)	—
"	5.640	2.94(17)	2.8(2)	—
"	5.650	3.25(17)	3.1(4)	—
"	5.660	3.5(3)	3.5(4)	—
"	5.665	4.03(16)	4.2(5)	—
"	5.670	4.8(2)	4.7(4)	—
"	5.675	6.0(4)	5.9(7)	—
"	5.680	6.3(3)	6.1(6)	—
"	5.685	7.7(4)	7.7(7)	—
"	5.690	9.3(7)	8.8(1.1)	—
"	5.695	—	6(2)	0.08(3)
"	5.700	—	4(2)	0.10(4)
"	5.710	—	2.3(5)	0.138(8)
"	5.720	—	2.1(5)	0.158(9)
"	5.730	—	2.5(5)	0.162(4)
$12^2 \times 48 \times 4$	5.675	5.6(5)	5.1(7)	—
"	5.680	6.8(6)	6.3(8)	—
"	5.685	8.6(6)	9.0(1.3)	—
"	5.690	13.4(1.3)	13.0(1.9)	—
"	5.695	—	3.9(1.4)	0.115(11)
$16^2 \times 64 \times 4$	5.690	16(2)	16(4)	—

Table 1

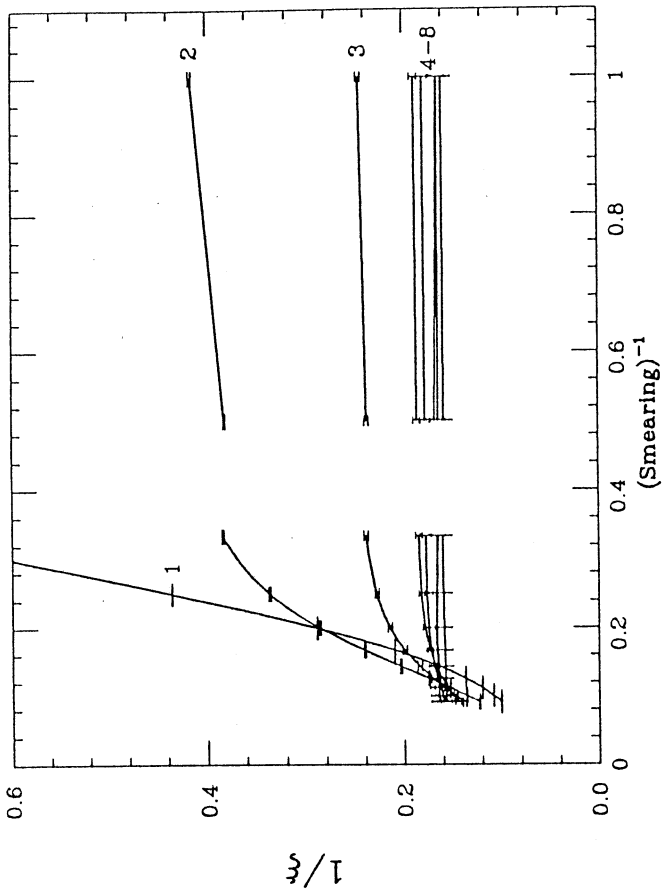

Fig. 1

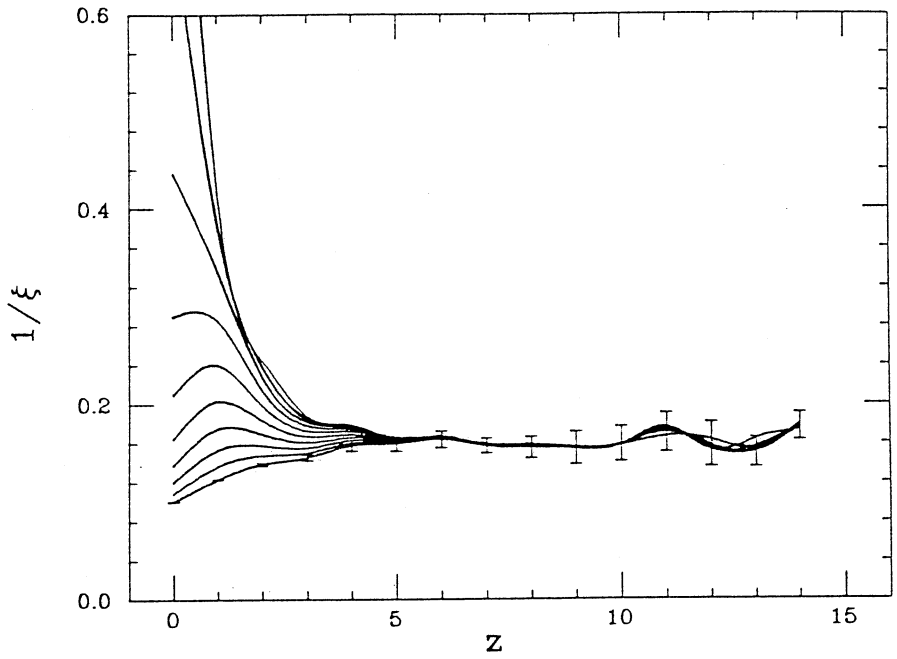

Fig. 2

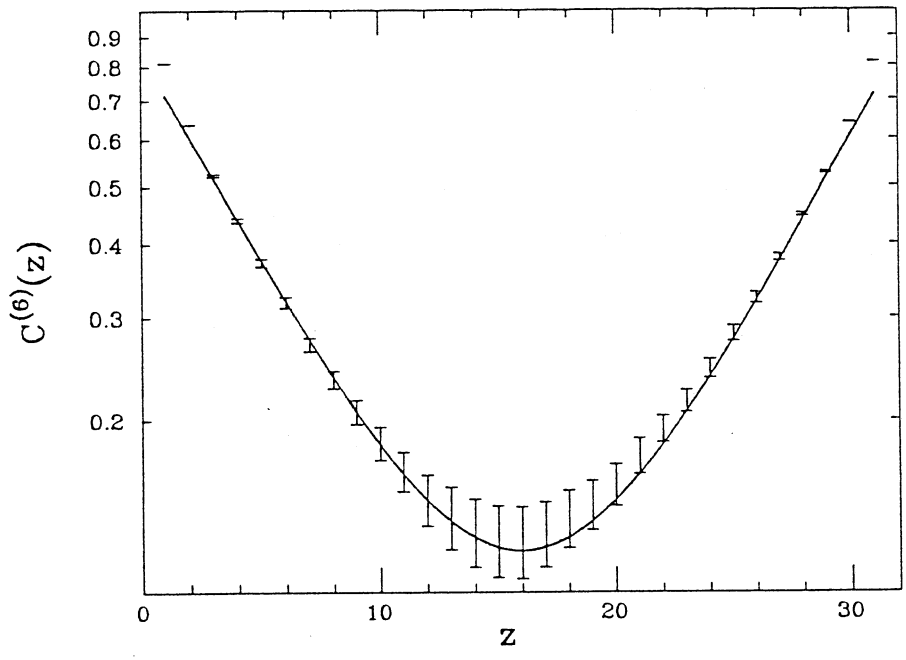

Fig. 3

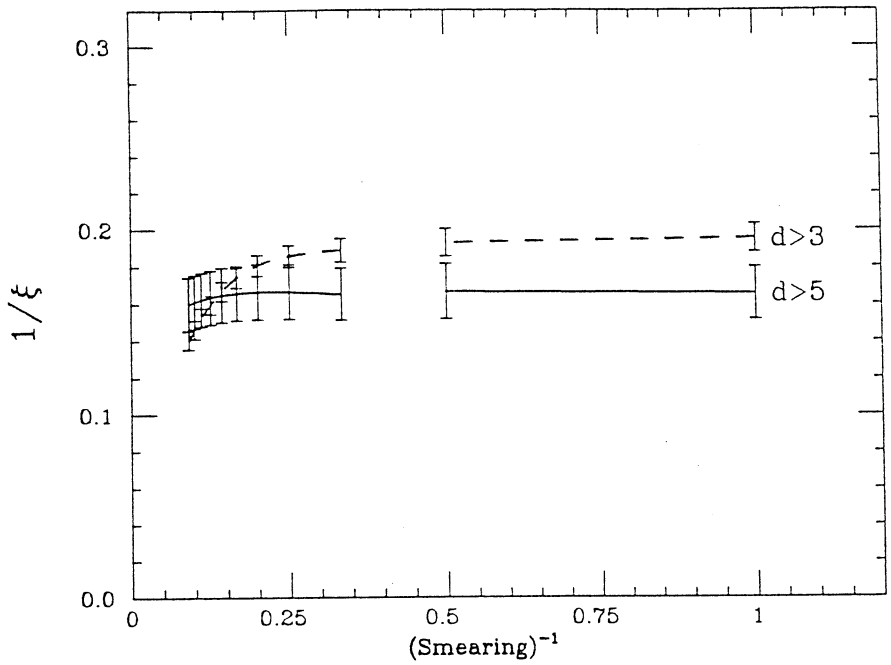
0.3
0.2
0.1
0.0
1/ξ
d>3
d>5
0
0.25
0.5
0.75
1
(Smearing)$^{-1}$

Fig. 4

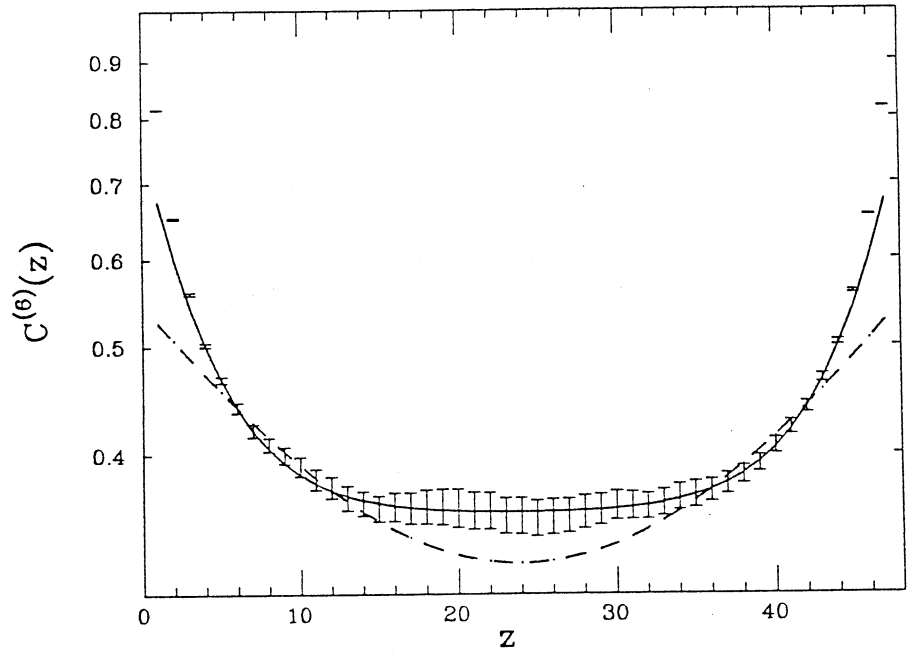
0.9
0.8
0.7
0.6
0.5
0.4
$C^{(6)}(z)$
0
10
20
30
40
z

Fig. 5

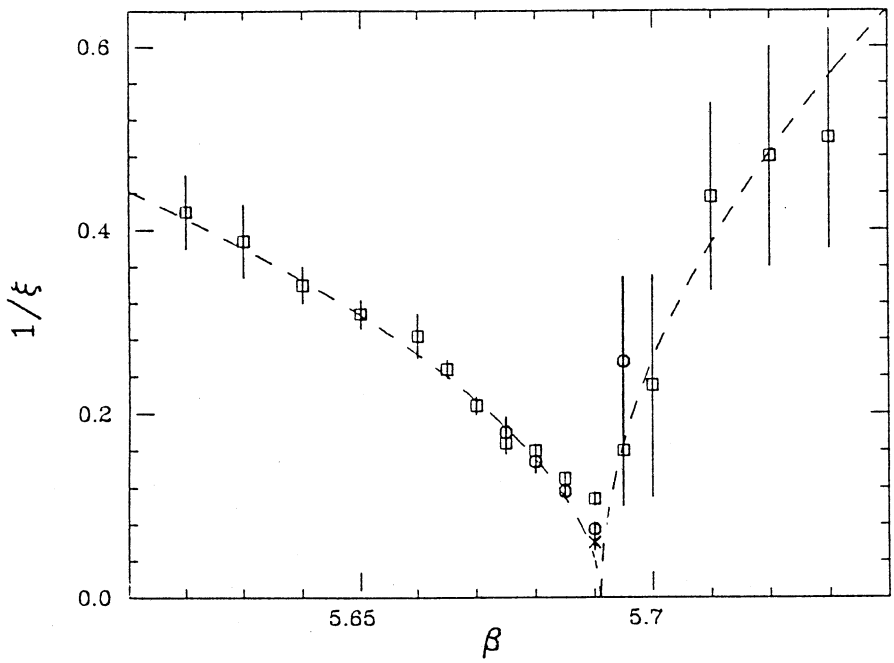
0.6
0.4
0.2
0.0
1/ξ
5.65
5.7
β

Fig. 6

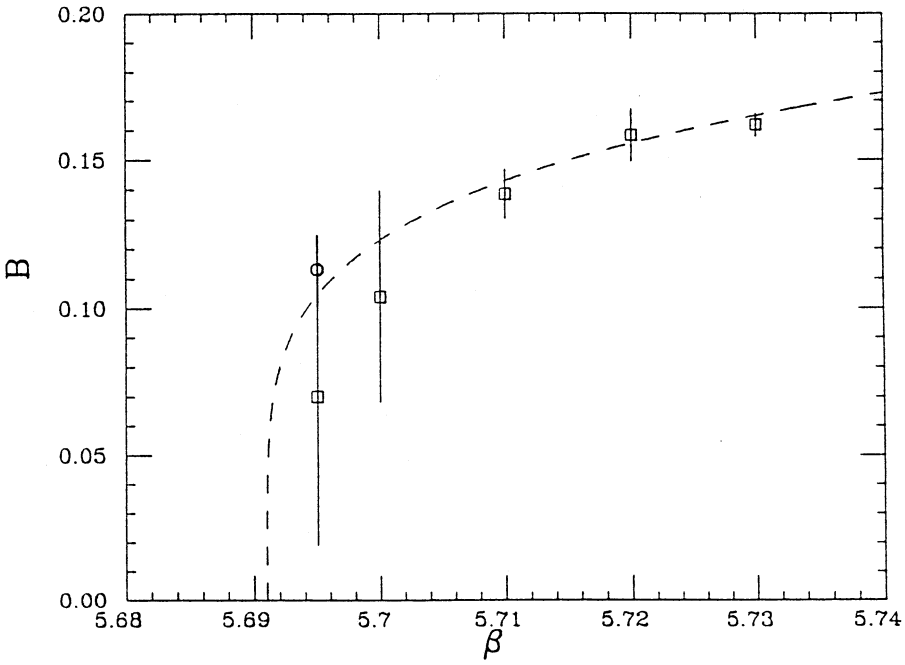
0.20
0.15
0.10
0.05
0.00
B
5.68
5.69
5.7
5.71
5.72
5.73
5.74
β

Fig. 7

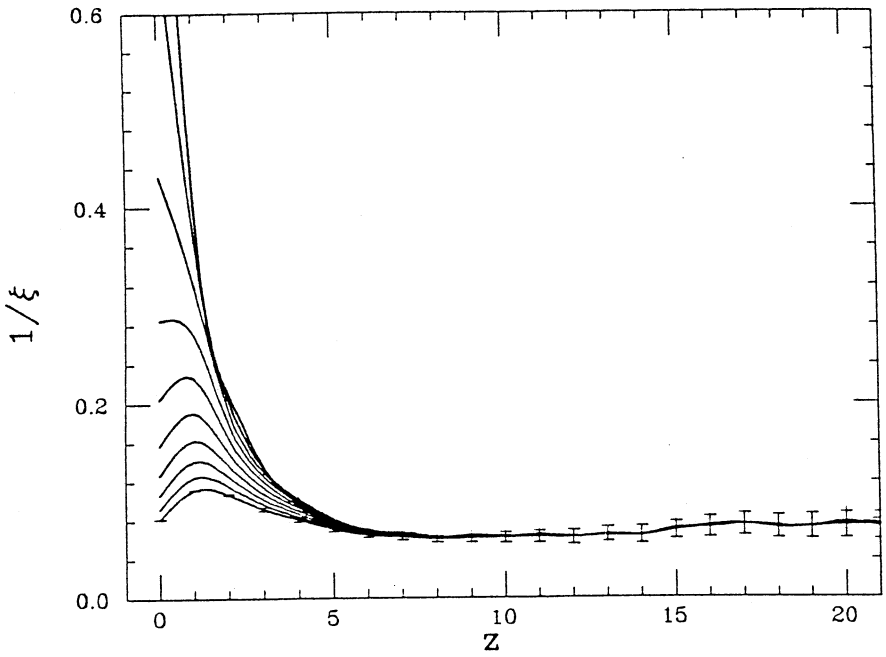

Fig. 8

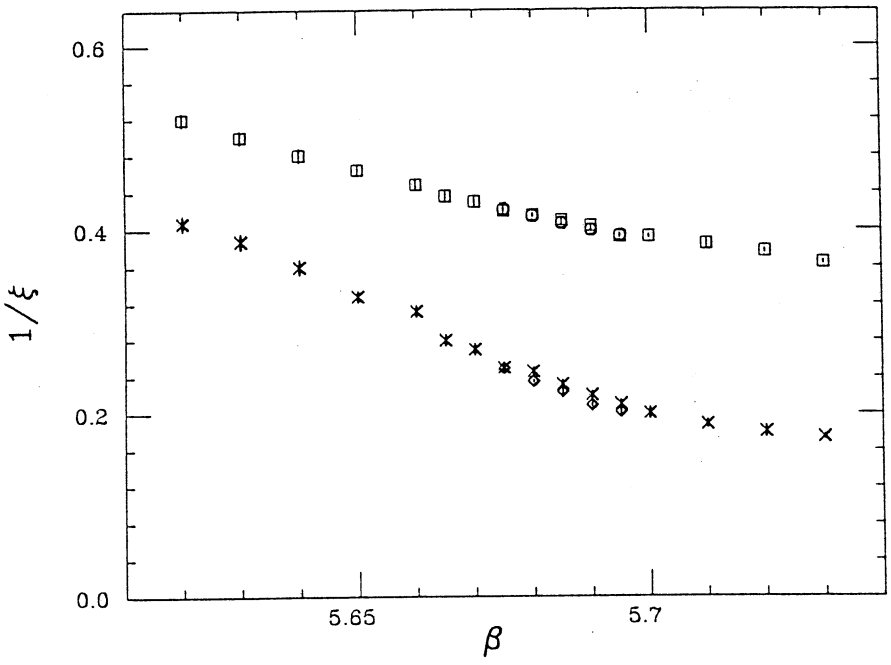

Fig. 9

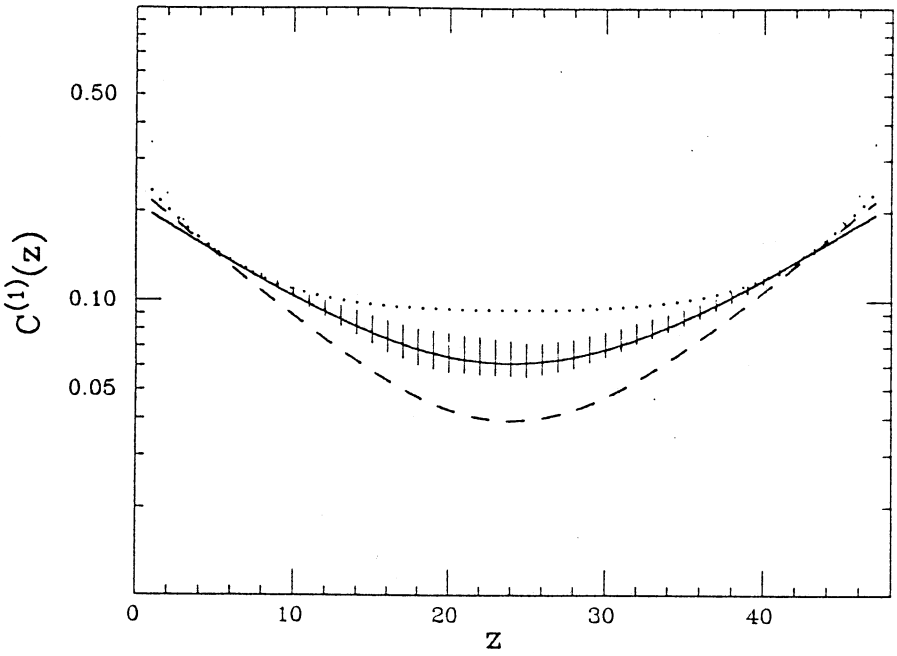

Fig. 10

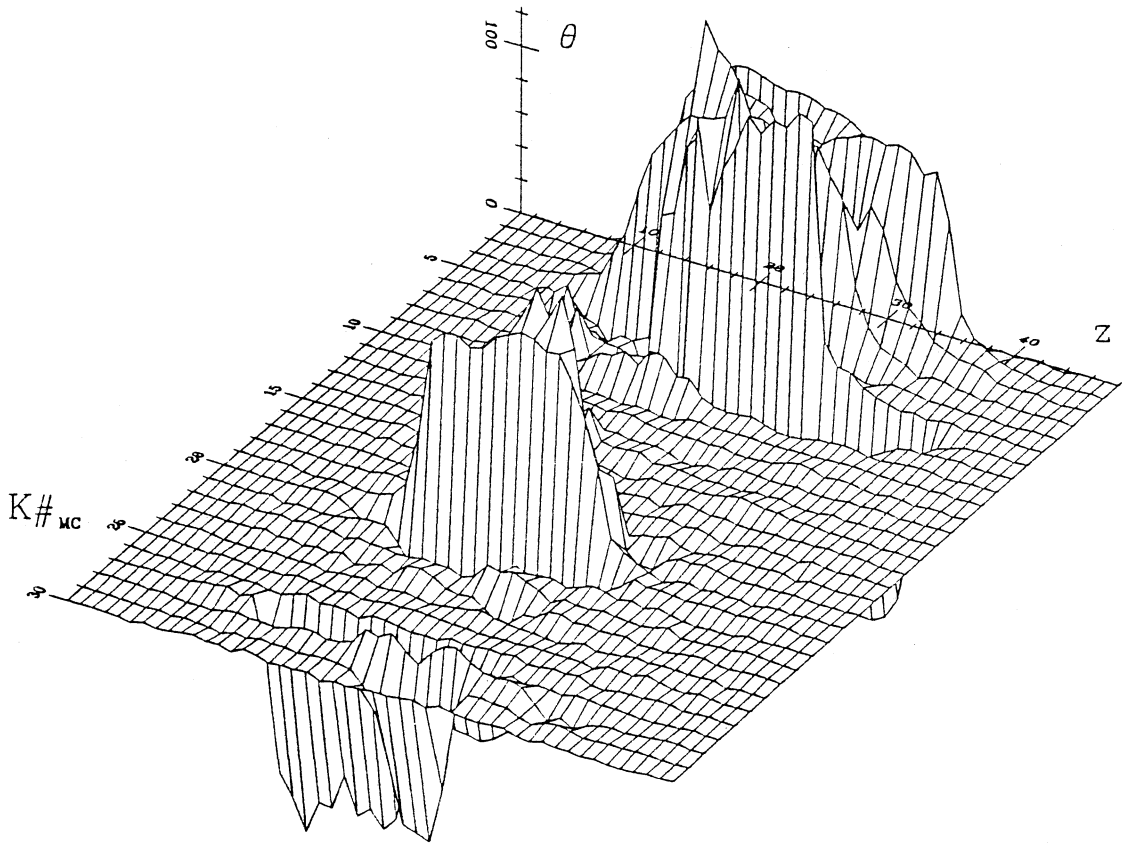

Fig. 11

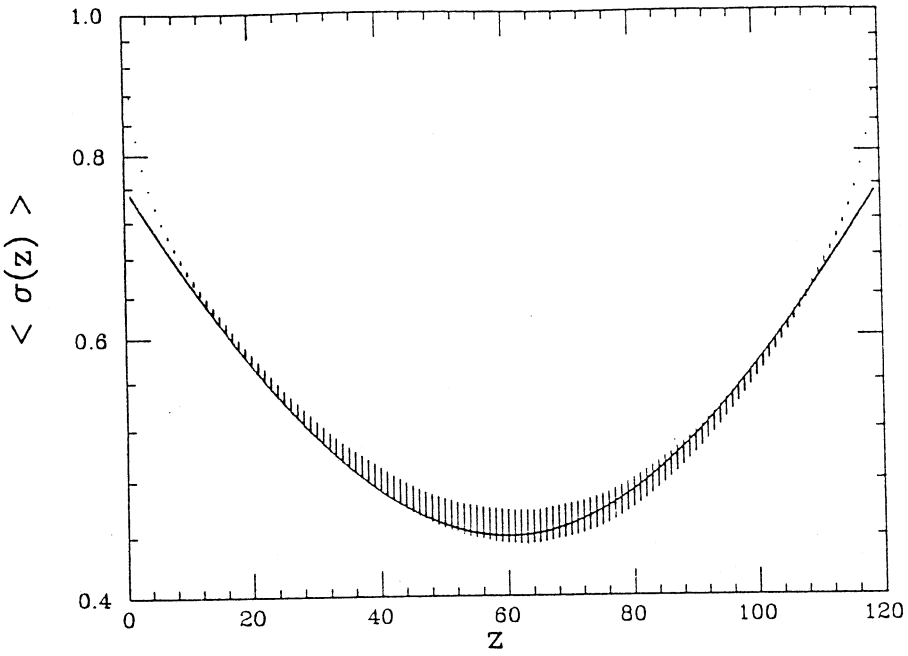
1.0
0.8
0.6
0.4
< σ(z) >
0
20
40
60
80
100
120
z

Fig. 12

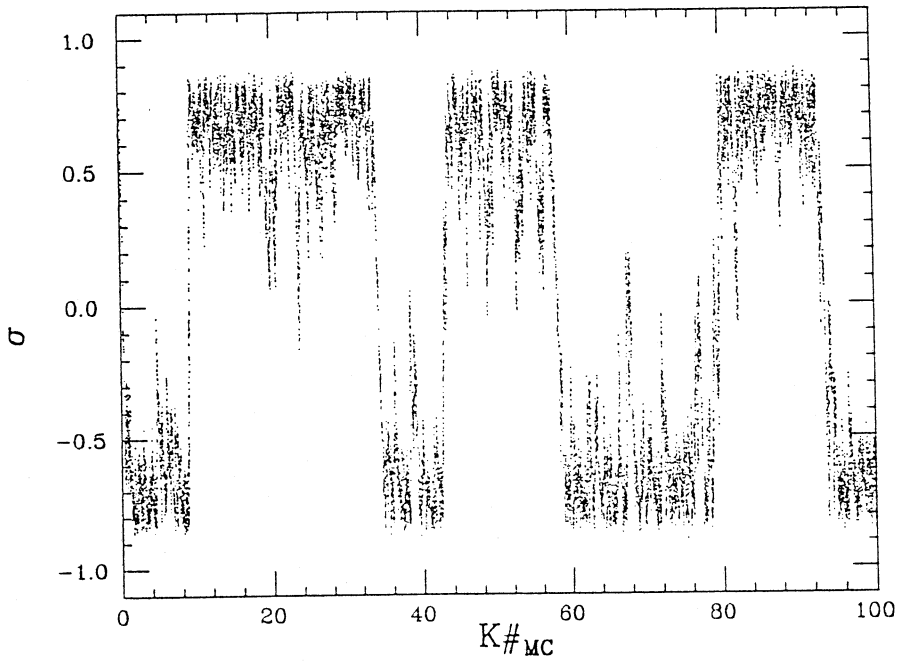
1.0
0.5
0.0
−0.5
−1.0
σ
0
20
40
60
80
100
K#MC

Fig. 13